Agricultural and Forest Meteorology 391 (2026) 111525

Contents lists available at ScienceDirect

Agricultural and Forest Meteorology

journal homepage: www.elsevier.com/locate/agrformet

Moso bamboo expansion impacts on root respiration of Japanese cedar forest and secondary broad-leaved forest in a socio-ecological production landscape

Kousuke Nagai [a], Si Ho Han [b,c,*], Dongchuan Fu [d,a], Hayato Abe [e], Tomonori Kume [e]

[a] Graduate School of Bioresource and Bioenvironmental Sciences, Kyushu University, Fukuoka, 819-0395, Japan
[b] Division of Environmental and Forest Science, College of Agriculture and Life Sciences, Gyeongsang National University, Jinju, 52828, Republic of Korea
[c] Institute of Agriculture and Life Science, Gyeongsang National University, Jinju, 52828, Republic of Korea
[d] Henan Academy of Forestry, Zhengzhou, 450008, China
[e] Kasuya Research Forest, Kyushu University, Sasaguri, Fukuoka, 811-2415, Japan

ARTICLE INFO

Keywords:
Phyllostachys edulis
Soil coring
Soil temperature
Soil CO_2 efflux
Autotrophic respiration
Shapley-based contribution analysis

ABSTRACT

Soil respiration and its root-derived component are important pathways for carbon release from forest ecosystems, but they remain poorly understood in expanding bamboo forests. We quantified root respiration and its drivers in an abandoned Moso bamboo forest (BF), a Japanese cedar forest (CF), and a mixed evergreen and deciduous broad-leaved forest (DF) in southwestern Japan during eight campaigns from April 2024 to March 2025. Using soil coring, we measured respiration from extracted living roots (R_a) together with fine- and coarse-root biomass. Nonlinear mixed-effects models describing R_a responses to soil temperature (T_s) and soil moisture (θ) were constructed. Mean R_a was highest in BF (0.285 g CO_2 m^{-2} h^{-1}), followed by DF (0.255 g CO_2 m^{-2} h^{-1}) and CF (0.057 g CO_2 m^{-2} h^{-1}). Fine-root temperature sensitivity and mass-specific respiration were lower in BF, indicating that physiological activity alone did not explain the elevated R_a. Instead, R_a was strongly influenced by fine-root biomass, which was approximately three times greater in BF than in DF and fifteen times greater than in CF. As a result, biomass-driven enhancement increased R_a in BF relative to CF, whereas lower mass-specific respiration in BF offset its biomass advantage over DF. Shapley-based contribution analysis supported these interpretations by revealing that fine-root biomass was the dominant positive driver of differences in R_a, whereas physiological factors partly offset the biomass effect. These local comparisons highlight that root respiration is shaped by combined biomass and physiological effects, whose relative importance differs among adjacent forest stands.

1. Introduction

Maximizing carbon (C) sequestration by forest ecosystems is a critical management objective to mitigate climate change (Pan et al., 2011). This objective is relevant to natural landscapes and socio-ecological production landscapes (SEPLs). The latter are defined as mosaics of distinct ecosystem types, shaped by long-standing human–nature interactions for the provision of ecosystem services (Duraiappah, 2012). Forests in SEPLs are characterized by a patchwork of diverse non- or semi-natural forest types, including plantation forests and natural secondary forests, which are utilized for different resources, such as wood, food, and organic fertilizer (Takeuchi et al., 2016). Furthermore, these forest patches fluctuate temporally and spatially owing to anthropogenic land-use changes and natural vegetation expansion (Zhang et al., 2024). Therefore, to achieve a balance between sustainable resource utilization and C sequestration in forested SEPLs, it is essential to understand C sequestration at the patch level with consideration of the vegetation dynamics.

One current challenge concerning SEPLs is their underuse, driven by rural depopulation and aging, resulting in a disconnection from nature (Soga and Gaston, 2016). In East Asia, SEPLs constitute a large proportion of the land coverage (Natori and Hino, 2021). Bamboo forest is an important landscape element in SEPLs together with natural secondary mixed forests and artificial plantations. Bamboo is the

* Corresponding author at: Division of Environmental and Forest Science, College of Agriculture and Life Sciences, Gyeongsang National University, Jinju 52828, Republic of Korea.
E-mail addresses: bupleurumhan@gmail.com, han.show.228@gnu.ac.kr (S.H. Han), fudongchuan127@163.com (D. Fu).

https://doi.org/10.1016/j.agrformet.2026.111525
Received 29 January 2026; Received in revised form 30 August 2026; Accepted 7 October 2026
Available online 16 October 2026
0168-1923/© 2026 The Authors. Published by Elsevier B.V. This is an open access article under the CC BY license (http://creativecommons.org/licenses/by/4.0/).

vernacular name for a subfamily of woody grasses in the family Poaceae. Bamboos are widely distributed, growing naturally in tropical and subtropical regions on all continents except Europe and Antarctica (Clark et al., 2015). Moso bamboo (*Phyllostachys edulis*) is a monopodial species that dominates a major forest type in East Asia. This species is native to southern China and was introduced to neighboring regions to provide food and other resources, and exhibits rapid growth and clonal reproduction (Benton, 2015). However, its utilization has declined in recent decades (Torii, 2003, 1998; Torii and Isagi, 1997). Consequently, its underuse has led to the abandonment of bamboo forest and its subsequent expansion into adjacent ecosystems (Isagi and Torii, 1997; Nishikawa et al., 2005; Suzuki and Nakagoshi, 2011).

Changes in forest patches can significantly alter the C cycle of an ecosystem (Jiao et al., 2024; Ma et al., 2017). Expansion of Moso bamboo forest into the surrounding forest could increase aboveground productivity (Yen et al., 2010). Moso bamboo forest is indicated to show a high C sequestration ability compared with that of the surrounding original forest types (Forster et al., 2025; Lin et al., 2017). However, research on belowground C dynamics—specifically, soil respiration—remains limited compared with that on aboveground components. Consequently, the differences in R_s among underused bamboo forest and the surrounding forest are poorly understood. Belowground C dynamics represent a major C flux (Raich and Schlesinger, 1992). Therefore, bridging this knowledge gap is crucial to understand the impacts of bamboo expansion on the C dynamics of SEPLs and to maximize the landscape-level C sequestration ability in SEPLs.

Soil respiration (R_s) is composed of autotrophic respiration from the roots (R_a) and heterotrophic respiration from soil-borne organisms (R_h). As bamboo is known for its extensive root system and high root biomass (Fukushima et al., 2015; Tang et al., 2015), the expansion of bamboo forest into surrounding forest is expected to increase R_s through the increment of R_a (Huang et al., 2021; Kuzyakov and Larionova, 2005). Indeed, bamboo forest often exhibits significantly higher R_s and R_a compared with those of coniferous forest and broad-leaved forest (Hu et al., 2018; Shi et al., 2015). However, Moso bamboo forest may show almost identical or lower R_s compared with that of the surrounding forest ecosystem (Hsieh et al., 2016; Liu et al., 2011). The mechanism of increment in R_a and R_s in Moso bamboo forest remains unclear because R_a is influenced by root quantity, the proportional composition of different root types (i.e., coarse- vs. fine-roots) (Jarvi and Burton, 2020; Pregitzer et al., 1998), and the sensitivity of root respiration to environmental factors (Jiang et al., 2013; Mauritz and Lipson, 2021; Thurgood et al., 2014). Although some reports indicate that these parameters differ among vegetation types (Cui et al., 2021; Hirano et al., 2023), such analyses have not been performed on expanding bamboo forest and the surrounding forest.

Several approaches can be used to evaluate R_a (Bouma et al., 1997; Kuzyakov and Larionova, 2005). The most commonly used conventional method is the trenching method, which involves digging a trench around a measurement plot and installing a barrier to preclude external roots from entering the plot (Ewel et al., 1987; Hirano et al., 2023; Jassal and Black, 2006). The respiration measured within this isolated plot is considered to be solely R_h. The R_a is estimated by subtracting the measured R_h value from the R_s measured in an adjacent, nontrenched control plot (Jassal and Black, 2006; Li et al., 2018). A key limitation of the trenching method, however, is that it does not provide information on root biomass at each measurement interval. Thus, this method is unsuitable for evaluation of the respective contributions of root quantity, root composition, and environmental sensitivity to changes in R_s and R_a. Alternatively, the soil core method, which involves the extraction of intact soil cores from the field (Cui et al., 2021; Kuzyakov, 2006; Li et al., 2018), enables the measurement of R_s from the core, after which the roots can be separated, and R_a and root biomass can be directly determined. This technique may provide initial insights into the mechanisms by which bamboo expansion into adjacent forest may increase R_s and R_a.

This study was conducted to evaluate (1) whether abandoned Moso bamboo forest has higher R_s and R_a than the surrounding forest types, comprising a Japanese cedar plantation and a secondary broad-leaved forest, and (2) whether the difference in R_a is driven by root biomass, root type, or sensitivity to environmental factors. To address these aims, we conducted 12-month field study in an abandoned Moso bamboo forest and adjacent Japanese cedar and secondary broad-leaved forests in northern Kyushu (Shinohara et al., 2014). Using the soil core method, we measured R_s and R_a to clarify the inter-stand differences to provide insights into the mechanisms driving R_a variation.

2. Methods

2.1. Study site

This study was conducted in an abandoned Moso bamboo forest (BF), a Japanese cedar plantation (CF), and a secondary mixed evergreen and deciduous broad-leaved forest (DF) in the Kasuya Research Forest of Kyushu University, Sasaguri, western Japan (33°37'N, 130°32'E) (Fig. 1a, b). The study site has a temperate climate and, according to data from a weather station in the Kasuya Research Forest located 3.5 km west of the study site, the mean annual temperature is 16.6 °C and the mean annual rainfall is 1794 mm (Fig. S1a, b; Yamauchi et al., 2026). The study site was situated on a single steep northeast-facing slope (~40°) at an elevation of 180–240 m. The underlying parent material is Sangun metamorphic rock. The soil is classified as a Cambisol based on the World Reference Base for Soil Resources (Anjos et al., 2015), which corresponds to Andic Brown Forest Soil in the Japanese soil classification system (Ichihashi et al., 2015; Shinohara et al., 2019).

2.2. Stand characteristics

The three forest stands were located along the same slope, enabling direct comparison under similar topographic conditions (Fig. 1b–e). The stand characteristics were measured and certain data were obtained from Shimono et al. (2022) and Ichihashi et al. (2017). The characteristics are summarized in Table 1.

The BF was an abandoned pure Moso bamboo (*Phyllostachys edulis*) forest with few understory herbs. Although the exact year is uncertain, the BF was established before 1969 and has not been actively managed in recent decades, based on checking the aerial photographs from the Geospatial Information Authority of Japan (Fig. S2). The culm density was 7900 culms ha^{-1} and culm diameter at breast height (DBH) was 9.8 cm. The canopy height was 12 m and the leaf area index (LAI) was 1.03 (Table 1).

The CF was a monospecific plantation of *Cryptomeria japonica*. The CF stand was established between 1951 and 1956 and has remained unmanaged since 1980. The CF understory comprised *Machilus thunbergii, Neolitsea sericea, Cinnamomum yabunikkei, Aucuba japonica*, and *Premna microphylla*. Understory species were not included in the present observations because their total basal area was <5% of that of the trees. The stem density was 1070 trees ha^{-1} and stem DBH was 34.1 cm. The canopy height was 25 m and the LAI was 1.75 (Table 1).

The DF was a secondary forest of mixed evergreen and deciduous broad-leaved trees dominated by *Quercus glauca, Machilus thunbergii, Cinnamomum camphora*, and *Quercus serrata*. Major natural or anthropogenic disturbances in the DF have not been recorded for >80 years. The stem density was 2970 trees ha^{-1} and stem DBH was 14.7 cm. The community height measured in 2025 was 16 m and the LAI was 2.83 (Table 1).

2.3. Measurement

A line-transect design was used to compare soil respiration among the forest types on montane slopes. In April 2024, five 10-m-long

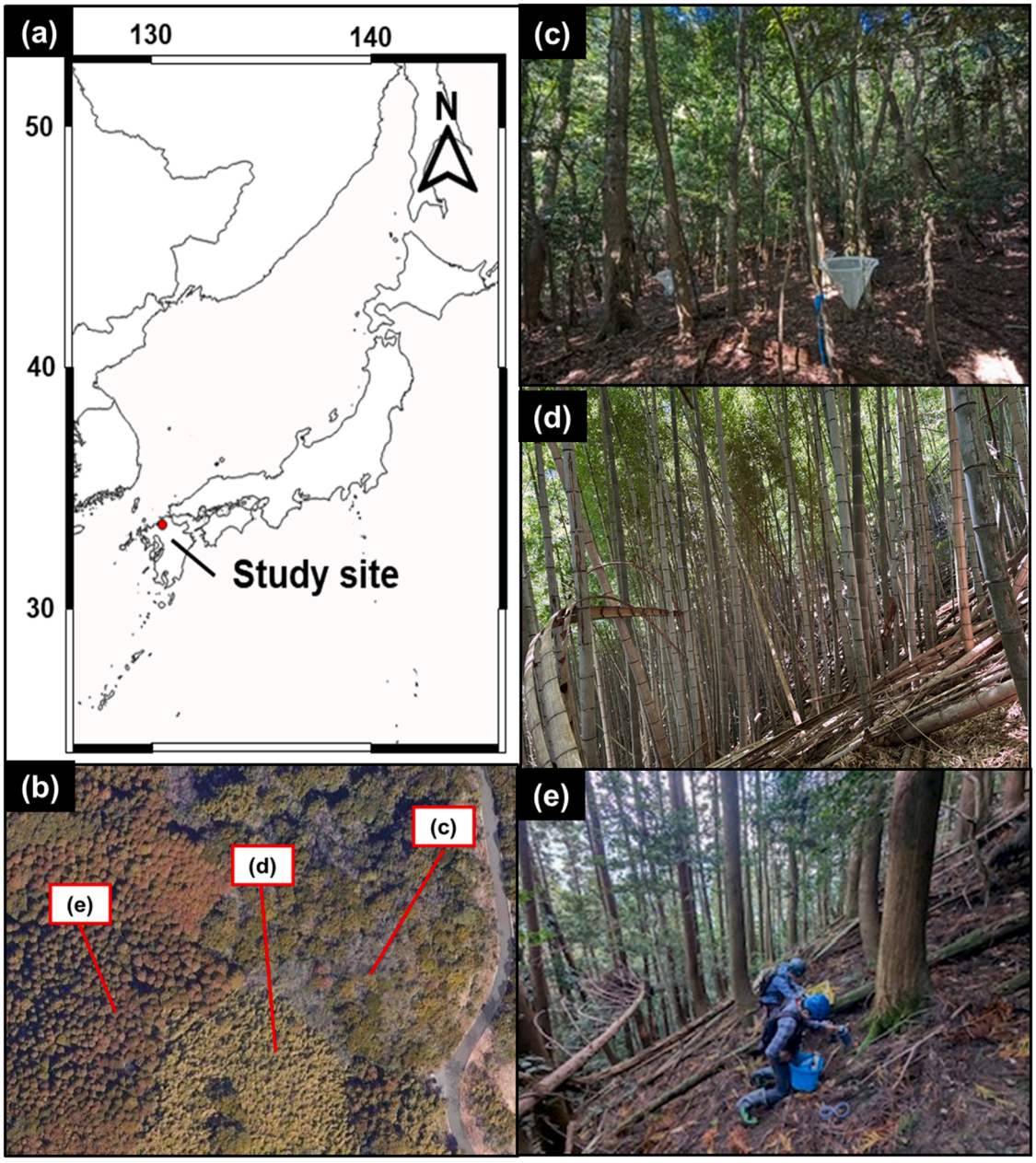


Fig. 1. Location of the study site (a), aerial photograph of the study site (b), and the forest types at the study site (c–e). In panel (a), the numbers along the upper and left margins indicate longitude (°E) and latitude (°N), respectively. In panel (c), secondary mixed evergreen and deciduous broad-leaved forest (DF), mainly composed of *Quercus glauca, Machilus thunbergii*, and *Cinnamomum camphora*. In panel (d), moso bamboo (*Phyllostachys edulis*) forest (BF). In panel (e), Japanese cedar (*Cryptomeria japonica*) forest (CF). The image in panel (b) was obtained from Google Earth (https://maps.app.goo.gl/cQvXCqnxapKdgsXR6).

transects were established along the altitudinal gradient of single slopes in each of the BF, CF, and DF (15 line transects in total). Transects within each forest were spaced at least 10 m apart. In each measurement campaign, one point per transect was selected for measurement of total soil respiration (R_s) and autotrophic respiration (R_a). Field measurements were conducted in eight campaigns from 19 April 2024 to 13 March 2025, in April, June, July, August, September, November, and December 2024, and March 2025. Measurements were generally conducted at intervals of 1–2 months, except for the longer interval between December 2024 and March 2025.

2.3.1. Soil respiration (R_s)

We measured R_s using two portable CO_2 gas analyzers (EGM-4 and EGM-5, PP Systems, Amesbury, MA, USA) based on a closed-chamber method. The R_s was measured three times for each measurement and the mean was used for data analyses. Polyvinyl chloride (PVC) collars were installed 1 month prior to the R_s measurement, with spacing of at least 1 m along the line transect. The PVC collar diameter of 10 cm and height of 2 cm were designed to fit the chamber size. Each PVC collar had four thin needles (3.2 cm long) that allowed insertion into the soil with minimal disturbance. At each R_s measurement point, the soil temperature (T_s) and soil moisture content (volumetric water content; θ) were measured. The T_s was measured once using a geothermometer (TST-9215A, Trusco Nakayama Corporation, Japan). The θ was measured three times using a soil moisture meter (Delta-T Devices, Cambridge, UK) and the average was calculated.

2.3.2. Root respiration (R_a) and root biomass

In this study, we assumed that total R_s comprised the sum of root respiration (R_a) and heterotrophic respiration (R_h) (Eq. (1)):

Table 1
Stand characteristics and soil properties for each forest type. The characteristics were recorded for each forest type from April 2024 to March 2025. Values are the mean (±SD) for each forest type. Moso bamboo forest (BF), Japanese cedar forest (CF), secondary mixed evergreen and deciduous broad-leaved forest (DF), leaf area index (LAI).

Forest type	BF	CF	DF
Dominant tree species	*Phyllostachys edulis*	*Cryptomeria japonica*	*Quercus glauca* Thunb. [a] *Machilus thunbergii* [a] *Cinnamomum camphora* [a]
Stem density (no. ha^{-1})	7900 (890) [b]	1070 (210) [b]	2970 (250) [a]
Stem diameter (cm)	9.8 (0.6) [b]	34.1 (0.7) [b]	14.7 (2.4) [a]
Canopy height (m)	12 (3)	25 (1)	16 (1)
LAI (in May) (m^2 m^{-2})	1.03 (0.41)	1.75 (0.28)	2.83 (0.44)
Soil pH	5.66 (0.10)	5.74 (0.18)	5.10 (0.52)
Soil carbon content (%)	5.13 (1.23)	5.39 (2.04)	6.90 (1.78)
Soil nitrogen content (%)	0.48 (0.09)	0.41 (0.08)	0.56 (0.08)
Soil bulk density (g cm^{-3})	0.31 (0.05)	0.34 (0.10)	0.27 (0.12)

[a] Data were obtained from Ichihashi et al. (2017).
[b] Data were obtained from Shimono et al. (2022).

$$R_s = R_a + R_h \quad (1)$$

The R_a was quantified directly using the soil core method (Burton et al., 1998; Majdi et al., 2007). After in situ R_s measurement, the soil at each measurement point was collected to a depth of 20 cm using a core sampler of diameter 10 cm, which was equivalent to the chamber diameter. The soil samples were collected in 0–10 cm and 10–20 cm subsamples. Roots and soil were sorted from the collected soil samples. The sorted roots were classified as living or dead based on visual indicators, including color, texture, and flexibility (An et al., 2017; Han et al., 2026; Vogt and Persson, 1991). Root segments with a faint to light brown exterior and some degree of flexibility were classified as living. Only living roots were used for respiration measurements and were separated into fine roots (<2 mm in diameter) and coarse roots (≥2 mm in diameter). In the BF, rhizomes were also visually identified during root sorting based on their characteristic morphology and separated from fine and coarse roots. The maximum diameter of the coarse roots recovered from the soil cores was 35.2 mm. Soil particles were washed off the sorted roots with water. The cleaned roots were placed in an empty cup and divided into fine-, coarse-roots and rhizomes. The cup (10.7 cm diameter, 9.6 cm height) comprised a PVC pipe with one end sealed using a polyethylene film and rubber tape. The gap between the chamber and the cup was sealed with putty and R_a was measured using portable CO_2 analyzers. We confirmed in advance that respiration of the empty cup was 0.00 g CO_2 m^{-2} h^{-1}. Measurement of R_a was performed within 3 h of collection of the soil samples. The duration of root sorting was fixed to 15 min because a preliminary survey conducted in March 2024 determined that >90% of the roots in any sample were sorted within 15 min. Thus, R_a in this study represents respiration measured from extracted living roots and does not include rhizosphere or mycorrhizal respiration. After R_a was determined, R_h was calculated by subtracting R_a from R_s.

To measure the fine- and coarse-root biomass (W) at each measurement point, the collected roots were dried in a constant temperature oven (DKN812, Yamato Scientific, Japan) at 70 °C for 48 h and the total dry weight was measured for each root type. In the BF, rhizomes were rarely encountered across the total 40 soil cores collected to a depth of 20 cm during the eight measurement campaigns. When rhizomes present, accounted for <3% of the measured R_a at each sampling point. Rhizomes were therefore excluded from the main analyses.

2.3.3. Continuous soil temperature monitoring

The T_s at 10 cm soil depth was recorded continuously at one measurement point per forest type using a soil temperature sensor (S-TMB-M002, HOBO, Onset Computer Corporation, Bourne, MA, USA) with a data logger (H21-USB, Onset Computer Corporation). Measurements were recorded at 30-min intervals from April 1, 2024, to March 31, 2025. However, in CF and DF, temperature data were not recorded from April 1, 2024, to May 27, 2024, and July 9, 2024, respectively. To substitute the missing data, we used T_s data recorded from the BF (T_{BF}) and applied linear regression-based conversion formulas to estimate the temperature in CF and DF. The conversions were based on relationships between T_{BF} and each forest type during the respective overlapping periods. The regression equations were as follows: $T_{CF} = 1.012 \times T_{BF} - 0.613$ ($R^2 = 0.993$) and $T_{DF} = 0.941 \times T_{BF} + 0.496$ ($R^2 = 0.994$), respectively.

2.4. Analysis

2.4.1. Comparison between forest types

To compare differences in R_s, its components (R_a and R_h), T_s, θ, fine-root biomass (W_f), and coarse-root biomass (W_c) among the forest types (BF, CF, and DF), we calculated the mean and standard deviation (SD) for each variable. For each forest type, the obtained mean corresponds to the temporal average across all sampling events and the SD reflects spatial variation among the five transects ($n = 5$). Dunnett's test was conducted in R software for windows ver. 4.3.3 (R Core Team, 2024) using the *glht* function of the "multcomp" package (Hothorn et al., 2008). BF was specified as the reference group in Dunnett's tests to directly evaluate the BF–CF and BF–DF contrasts. Because our primary objective was to evaluate potential impacts of bamboo expansion into the surrounding forest, the BF was treated as the baseline condition.

2.4.2. Response to environmental drivers

To evaluate the primary environmental drivers determining temporal changes in R_s and R_a, we examined the relationships of R_s, R_a, R_{a_c}, and R_{a_f} with T_s (Fig. S1c) and θ (Fig. S1d) for each forest type (BF, CF, and DF) in accordance with our previous studies (Abe et al., 2025; Hsieh et al., 2016). This analysis used three empirical equations. The first equation (Eq. (2)) expressed the exponential relationship using T_s (Lloyd and Taylor, 1994):

$$F = a \exp(bT_s) \quad (2)$$

where a and b are constants, and F is the respiration flux (g CO_2 m^{-2} h^{-1}). The second equation (Eq. (3)) expressed the quadric relationship using θ (Saiz et al., 2006):

$$F = c + d\theta + f\theta^2 \quad (3)$$

where c, d, and f are constants. The third equation (Eq. (4)) expressed the exponential power relationship using T_s and θ (Saiz et al., 2006):

$$F = g \exp(hT_s)\, \theta^i \quad (4)$$

where g, h, and i are constants. To determine the values of the constants in Eqs. (2)–4, non-linear mixed-effect models (Abe et al., 2025; Lindstrom and Bates, 1990) were applied to pooled data from the five measurement points for each forest type using R software with the package "nlme" (Pinheiro et al., 2022). All constants in Eqs. (2)–4 consisted of fixed and random effects, and the fixed effects were expressed as representative constants in each forest type. Random effects were assigned to differences in measurement points in each forest type. Constants were fitted using a maximum likelihood procedure. The goodness of fit was evaluated with the Akaike information criterion (AIC) and the coefficient of determination that quantified the variance explained by the fixed effects only (marginal R^2) (Spiess and Neumeyer,

2010) (Tables S1–S3).

2.4.3. Annual root respiration estimates

To estimate annual R_a, R_{a_c}, and R_{a_f}, the continuous T_s data were substituted into the fitted temperature-driven respiration models (Eq. (2)). The temperature-only model showed the lowest AIC for total R_a in all three forest types, while models including θ did not consistently improve models performance for R_a, R_{a_c}, and R_{a_f} across forest types (see Section 3.1, Tables S2 and S3). We therefore used the temperature-driven models to estimate annual R_a and its root-class components. Total annual R_a, R_{a_c}, and R_{a_f} were obtained by integrating the predicted fluxes over the year. The values represent the fixed-effect estimates of the models, and their spatial variation was evaluated using point-specific random effects. Predicted annual respiration was converted to mass-based units (g C m^{-2} yr^{-1}) using standard molar conversions.

2.4.4. Temperature sensitivity

To separate physiological temperature sensitivity from differences in root biomass in R_a, we evaluated root respiration normalized by root biomass ($R_{a_f}/W_{_f}$ and $R_{a_c}/W_{_c}$). To examine the temperature sensitivity of the root-biomass-specific R_a, we analyzed the relationship between T_s and R_a per unit root biomass for fine- and coarse-roots, respectively (i.e., $R_{a_f}/W_{_f}$ and $R_{a_c}/W_{_c}$). For each forest type, nonlinear regression models were fitted to the observed data using the exponential equation (Eq. (5)):

$$F = \mathrm{j}\ \exp\ (\mathrm{k}T_s) \quad (5)$$

In this context, F in Eq. (5) represents $R_{a_f}/W_{_f}$ or $R_{a_c}/W_{_c}$ (μmol CO_2 h^{-1} g^{-1}), and j and k correspond to the intercept and temperature-sensitivity coefficient, respectively. Model fitting was conducted in R using the package "nlraa" (Fernando, 2020). The parameters j and k were estimated using nonlinear least squares fitting. Confidence intervals (95%) for the fitted curves were calculated to assess the reliability of the parameter estimates. The quality of model fit was evaluated based on the coefficient of determination (R^2) (Table S4).

2.4.5. Shapley-based attribution of R_a differences among forest types

To clarify which factors most strongly contributed to the differences in annual R_a among the BF, CF, and DF, we conducted an attribution analysis based on the Shapley value framework (e.g., Wadoux, 2023). This approach allows the effects of multiple interacting variables—such as fine- and coarse-root biomass, their biomass-specific respiration parameters (a and b in Eq. (2)), and soil temperature—to be separated and quantified in terms of their contributions to inter-stand differences in R_a.

For each forest type, annual R_a was calculated as the sum of R_{a_f} and R_{a_c}, obtained by multiplying the biomass-specific respiration model (see Section 2.4.4) with the corresponding fine- and coarse-root biomass. To evaluate the degree that each parameter contributed to the R_a difference between two stands (i.e., between the BF and CF, and between the BF and DF), we replaced the baseline parameters sequentially with those of the comparison stand, considering all possible permutations. Averaging the marginal change in R_a across all permutations yielded an order-independent estimate of each parameter's contribution to the R_a differences between BF and CF, and between BF and DF. This analysis quantified the relative importance of root biomass ($W_{_f}$ and $W_{_c}$), physiological root traits (a and b for R_{a_f} and R_{a_c}, respectively), and the thermal environment (mean annual T_s) in explaining the R_a differences between BF and CF, and between BF and DF. The percentage contribution of each factor was calculated as its mean marginal change in annual R_a divided by annual R_a of the baseline stand and multiplied by 100. CF and DF were used as the baseline stands for the CF-to-BF and DF-to-BF comparisons, respectively. The Shapley decomposition was performed using Python for Windows version 3.11.

3. Results

3.1. Seasonal trends for soil temperature (T_s), soil moisture (θ), soil respiration (R_s), and root biomass

3.1.1. Soil temperature and soil moisture

Soil temperature (T_s) and soil moisture (θ) in BF, CF, and DF exhibited similar seasonal trends during the observation period (April 2024–March 2025), with the highest T_s and lowest levels of θ observed in summer (July–September 2024) (Fig. 2, Table S5, S6). The mean T_s in BF (mean ± SD, 18.0 ± 0.2 °C) was significantly higher than that in CF (17.6 ± 0.2 °C, $p < 0.05$) and DF (17.4 ± 0.2 °C, $p < 0.05$) (Table S6). Regarding θ, BF showed significantly lower values (21.3% ± 1.7%) compared with CF (28.2% ± 3.2%, $p < 0.05$), whereas no significant difference was detected between BF and DF (20.2% ± 1.46%, $p > 0.05$).

3.1.2. Soil respiration components (R_s, R_a, and R_h)

Higher R_s and R_a were observed in summer than during winter (December 2024–February 2025), and the amplitude of the peaks differed between the three stands (Fig. 2, S3). The mean R_s in BF (0.8 ± 0.4 g CO_2 m^{-2} h^{-1}) was significantly higher than that in CF (0.26 ± 0.03 g CO_2 m^{-2} h^{-1}, $p < 0.05$), whereas no significant difference was observed between BF and DF (0.4 ± 0.1 g CO_2 m^{-2} h^{-1}) (Table S6). The mean R_a in BF (0.29 ± 0.06 g CO_2 m^{-2} h^{-1}) was significantly higher than that in CF (0.06 ± 0.02 g CO_2 m^{-2} h^{-1}, $p < 0.05$), whereas no significant difference was observed between BF and DF (0.26 ± 0.04 g CO_2 m^{-2} h^{-1}) (Table S6). The mean fine-root respiration (R_{a_f}) in BF (0.23 ± 0.05 g CO_2 m^{-2} h^{-1}) was significantly higher than in CF (0.023 ± 0.01 g CO_2 m^{-2} h^{-1}) and DF (0.16 ± 0.03 g CO_2 m^{-2} h^{-1}). In contrast, mean coarse-root respiration (R_{a_c}) in BF (0.06 ± 0.02 g CO_2 m^{-2} h^{-1}) was similar to that of CF (0.03 ± 0.02 g CO_2 m^{-2} h^{-1}) but significantly lower than that of DF (0.10 ± 0.02 g CO_2 m^{-2} h^{-1}). Heterotrophic respiration (R_h) showed no significant differences between BF (0.47 ± 0.35 g CO_2 m^{-2} h^{-1}) and the other forest stands, i.e., CF (0.20 ± 0.03 g CO_2 m^{-2} h^{-1}) and DF (0.21 ± 0.07 g CO_2 m^{-2} h^{-1}) (Table S6).

The seasonal patterns for R_s and R_a were predominantly regulated by T_s rather than θ in this study. The effect of θ on the reproducibility of R_s and R_a, as evaluated by the model fit (R^2 and AIC), was smaller than that of T_s, regardless of stand type (Tables S1–S3).

3.1.3. Root biomass

The total root biomass ($W_{_c} + W_{_f}$), representing the sum of coarse-root biomass ($W_{_c}$) and fine-root biomass ($W_{_f}$), was 0.21 ± 0.04 g cm^{-2} in BF, which was significantly higher than in CF (0.05 ± 0.02 g cm^{-2}, $p < 0.05$) but not significantly different from DF (0.17 ± 0.01 g cm^{-2}, $p > 0.05$) (Fig. 2, Table S6). Fine-root biomass ($W_{_f}$) in BF (0.15 ± 0.03 g cm^{-2}) was significantly higher than in CF (0.010 ± 0.003 g cm^{-2}, $p < 0.05$) and DF (0.05 ± 0.02 g cm^{-2}, $p < 0.05$). Regarding coarse-root biomass ($W_{_c}$), BF (0.07 ± 0.02 g cm^{-2}) showed significantly higher biomass than CF (0.03 ± 0.02 g cm^{-2}, $p < 0.05$), but significantly lower than DF (0.12 ± 0.02 g cm^{-2}, $p < 0.05$). Overall, the proportion of fine-root biomass relative to total root biomass was highest in BF (70%) compared with those in CF (22%) and DF (31%).

3.2. Differences in annual R_a across different forest types

Annual cumulative R_a, which was derived with T_s and the fitting models (Tables S1–S3), differed substantially among the three forest types (Fig. 3). The R_a was highest in BF (636.2 ± 249.1 g C m^{-2} yr^{-1}), followed by DF (568.6 ± 222.5 g C m^{-2} yr^{-1}), and was lowest in CF (118.3 ± 79.6 g C m^{-2} yr^{-1}). Among R_a components, the proportion of R_{a_f} was higher than R_{a_c} in BF (80.9%) and DF (62.2%), whereas CF showed a lower R_{a_f} proportion (40.7%) compared with R_{a_c}.

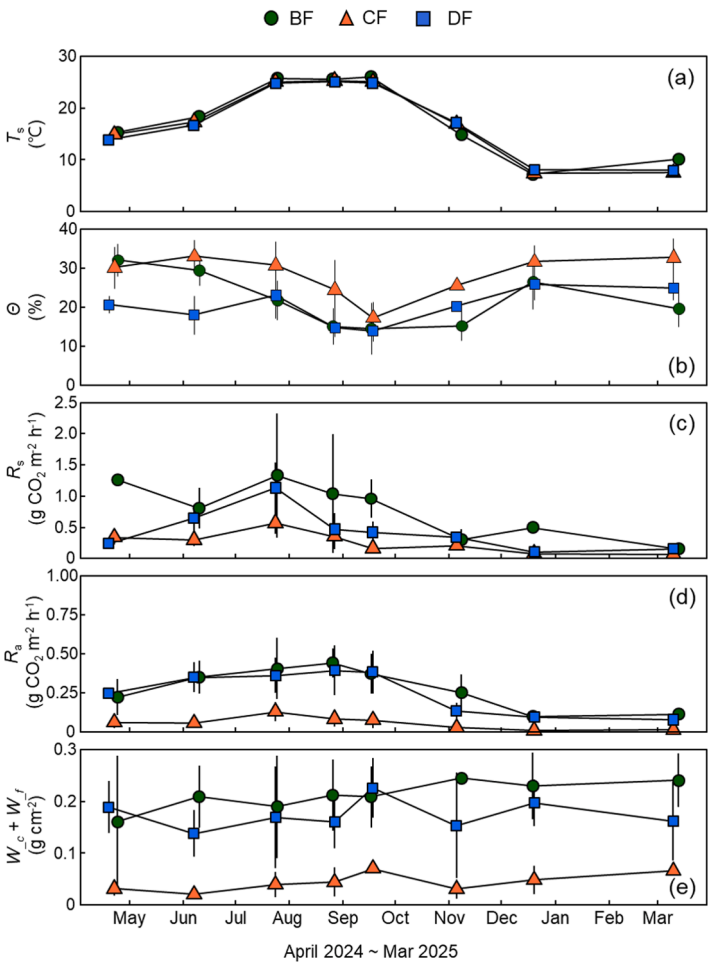


Fig. 2. Seasonal trends in (a) soil temperature (T_s), (b) soil volumetric water content (θ), (c) total soil respiration (R_s), (d) autotrophic respiration (R_a), and (e) total root biomass ($W_c + W_f$) in the three forest types from April 2024 to March 2025. The data represent means for each measurement campaign and vertical bars indicate the standard deviation across replicate transect lines ($n = 5$). Moso bamboo forest (BF), Japanese cedar forest (CF), secondary mixed evergreen and deciduous broad-leaved forest (DF).

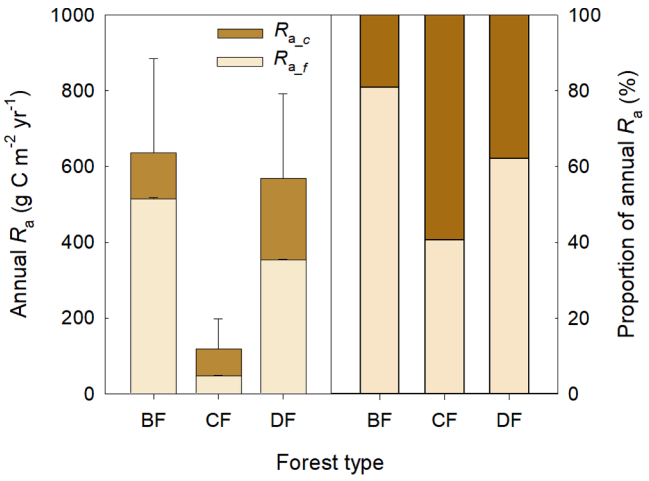


Fig. 3. Annual cumulative autotrophic respiration (R_a) in the three forest types from April 2024 to March 2025. R_a was calculated from the fixed effect ± SD of the random effect. R_{a_c} and R_{a_f} mean R_a of coarse- and fine root, respectively.

3.3. Responses of R_a per unit root biomass to T_s

The R_a per unit biomass increased exponentially with T_s in all forest types (Fig. 4). Fine-roots generally exhibited greater temperature sensitivity than coarse-roots, and greater temperature sensitivity was observed in CF and DF compared with BF. In BF, the temperature coefficient (k) for fine-roots was 0.074, similar to that for coarse-roots (0.086). In CF, fine-roots showed the highest sensitivity among all forest types (k = 0.097), together with a relatively high basal respiration rate (j = 0.728). In DF, fine-roots displayed the highest basal respiration (j = 1.139) combined with a relatively high temperature coefficient (k = 0.091). The Q_{10} values for the R_{a_f} per unit biomass in BF, CF, and DF were 2.10, 2.64, and 2.48, respectively. In contrast, coarse-roots consistently exhibited lower basal respiration rates (j = 0.358–0.449) than that of fine-roots and a similar temperature dependence (k = 0.078–0.099) to that of fine-roots.

3.4. Relative contributions of variables to R_a differences

The Shapley-based simple exercise showed that the W_f was the primary factor driving the higher annual R_a in BF compared with CF and DF, whereas other parameters, such as the temperature-sensitivity coefficients (j and k), exerted compensatory effects that reduced the differences in R_a among the forest types (Fig. 5a, b). The ~400% higher R_a in BF than in CF was largely attributable to the greater W_f in BF, whereas the temperature sensitivity of fine-roots (b) partly offset this effect (Fig. 5a). Similarly, the larger W_f in BF had the potential to generate ~80% higher R_a in BF than in DF; however, this positive effect of W_f was substantially offset by the temperature-sensitivity parameters

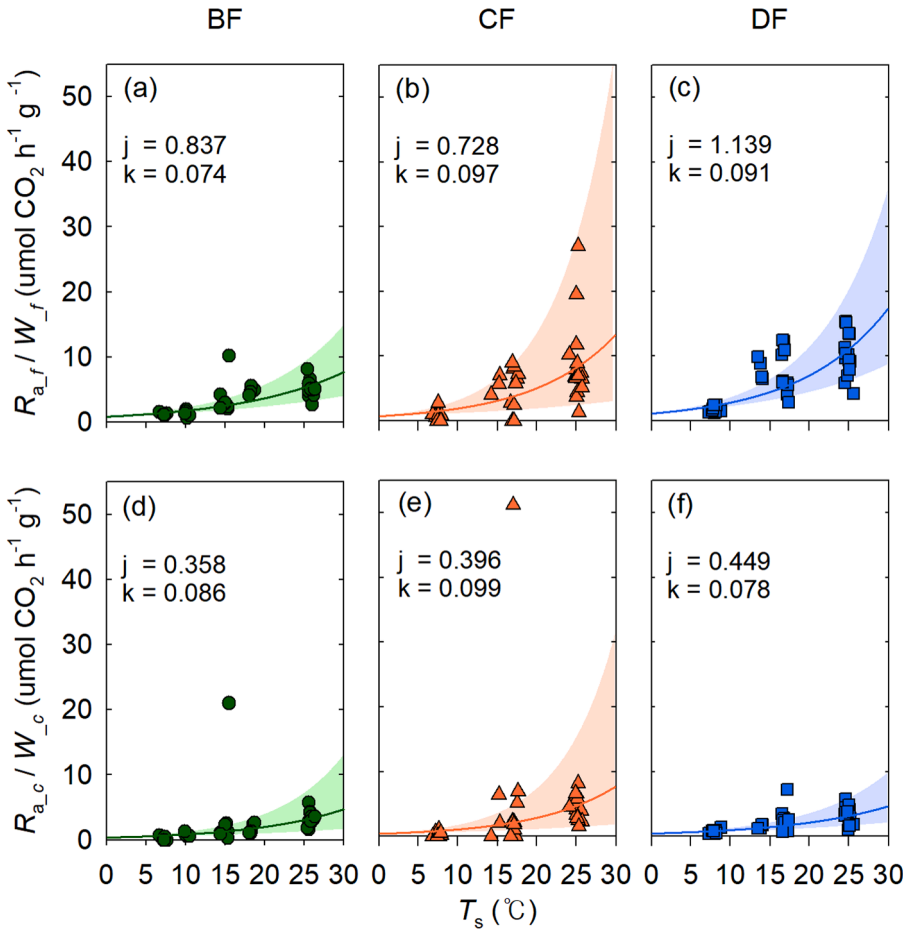


Fig. 4. Relationships between soil temperature (T_s) and root respiration per unit biomass in the three forest types. Panels (a–c) show fine-root respiration rates per unit fine-root biomass ($R_{a_f}/W_{_f}$), and (d–f) show coarse-root respiration rates per unit coarse-root biomass ($R_{a_c}/W_{_c}$). Each point represents one observation. The curves represent nonlinear regression lines fitted with the model $y = j \exp(k\ T_s)$. Shaded areas indicate the 95% confidence intervals for the nonlinear regression model. j and k are estimated coefficients.

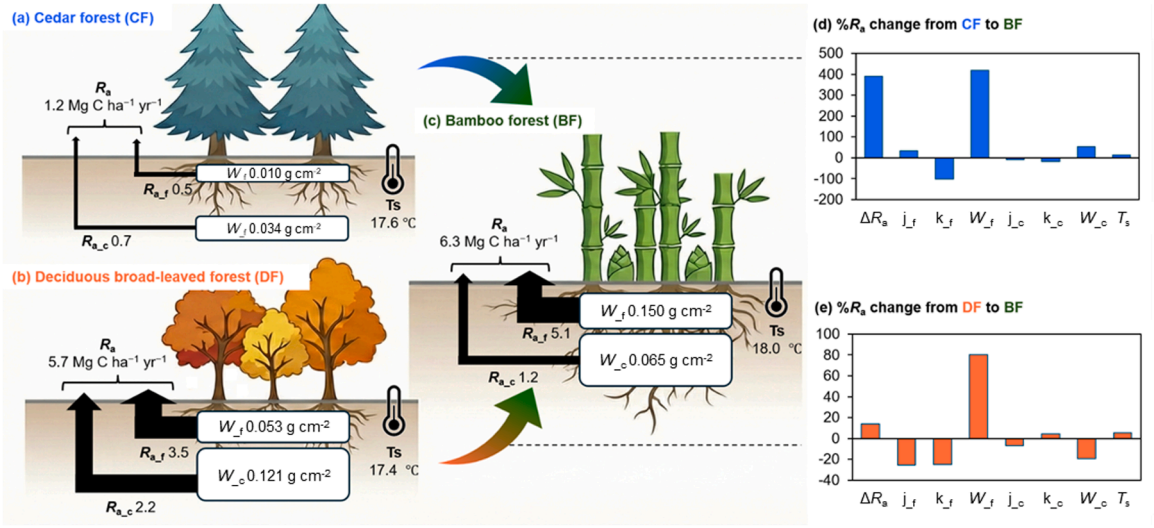


Fig. 5. Schematic diagram of the Shapley-based attribution procedure for percentage change in autotrophic respiration (R_a). Panels (a–c) show the annual cumulative values for R_a, fine-root R_a (R_{a_f}), and coarse-root R_a (R_{a_c}), as well as the mean values for fine-root biomass (W_f), coarse-root biomass (W_c), and soil temperature (T_s) in measurement campaigns in (a) Japanese cedar forest (CF), (b) secondary mixed evergreen and deciduous broad-leaved forest (DF), and (c) moso bamboo forest (BF). Panels (d and e) show the relative contribution of each factor affecting the percentage change in R_a from CF to BF (d) and from DF to BF (e). The parameters j_f and k_f are the scaling and temperature-sensitivity coefficients, respectively, of the R_{a_f}/W_f model; j_c and k_c are the corresponding coefficients of the R_{a_c}/W_c model. The horizontal reference line at 0 indicates no change in R_a.

of fine-roots (j and k) and by W_c, resulting in almost equivalent annual R_a between BF and DF (Fig. 5b). Although T_s differed significantly among forest types (Table S6), its contribution to the difference in R_a was <15% (~15% for BF and ~5% for DF in Fig. 5a and b, respectively).

4. Discussion

4.1. R_s and R_a among forest types

Average soil respiration rates varied among the three forest types. BF exhibited the highest mean R_s (0.772 g CO_2 m^{-2} h^{-1}), which was approximately three times greater than that of CF (0.257 g CO_2 m^{-2} h^{-1}) and almost double that of DF (0.446 g CO_2 m^{-2} h^{-1}) (Table S6). These results indicate that the bamboo stand maintained relatively high instantaneous CO_2 efflux during the measurement period, consistent with previous observations that unmanaged bamboo forests can exhibit elevated respiratory activity compared with other temperate forest ecosystems (Hsieh et al., 2016; Tang et al., 2016a).

The R_a showed even stronger contrasts across forest types. BF had a mean R_a of 0.285 g CO_2 m^{-2} h^{-1}, which was five times higher than CF (0.057 g CO_2 m^{-2} h^{-1}) and slightly higher than DF (0.255 g CO_2 m^{-2} h^{-1}) (Table S6). The elevated R_a in BF was primarily attributable to fine-root respiration, as R_{a_f} in BF (0.228 g CO_2 m^{-2} h^{-1}) was an order of magnitude greater than in CF (0.023 g CO_2 m^{-2} h^{-1}) and substantially higher than in DF (0.156 g CO_2 m^{-2} h^{-1}). This pattern is consistent with the markedly larger fine-root biomass in BF, which was approximately 15 times that of CF and almost three times that of DF (Ichihashi et al., 2015; Shimono et al., 2022). Although previous studies indicate that mass-specific respiration may be higher in tree-dominated stands, the substantial fine-root biomass in BF is indicated to exert a stronger influence on instantaneous R_a than mass-specific physiological properties alone (Cui et al., 2021; Hirano et al., 2023).

Collectively, these results suggest that the elevated instantaneous R_s and R_a in bamboo forest originate from the combination of high fine-root density and sustained root activity, reinforcing the viewpoint that unmanaged bamboo stands maintain inherently high belowground respiratory fluxes even at short temporal scales.

4.2. Factors associated with differences in R_a among forest types

Annual R_a was quantified separately for coarse-roots (R_{a_c}) and fine-roots (R_{a_f}) in each forest type (Fig. 3). Annual R_a was 6.3 Mg C ha^{-1} yr^{-1} in BF, 1.2 Mg C ha^{-1} yr^{-1} in CF, and 5.7 Mg C ha^{-1} yr^{-1} in DF. In BF, R_{a_f} accounted for approximately 81% of the total R_a, whereas R_{a_c} contributed 19%. In CF, R_{a_c} dominated R_a, contributing approximately 58%, whereas R_{a_f} accounted for 42%. DF showed an intermediate contribution structure, with R_{a_f} contributing 61% of R_a and R_{a_c} contributing 39%. These results demonstrate that the soil core method enables direct quantification of fine- and coarse-root contributions to R_a.

The foregoing values exceed those reported for low-density Moso bamboo plantations (2.1–4.3 Mg C ha^{-1} yr^{-1}) (Huang et al., 2021; Tang et al., 2016b; Tu et al., 2013), indicating relatively high root-derived respiratory CO_2 fluxes in the unmanaged bamboo stand (Deng et al., 2020; Xu et al., 2024). The R_a in BF also higher that of agricultural systems, where global cropland averages are approximately 3.7 Mg C ha^{-1} yr^{-1} (Jian et al., 2021) and maize fields typically range from 1.4 to 2.1 Mg C ha^{-1} yr^{-1} (Chen et al., 2017). These comparisons suggest that bamboo expansion within SEPLs may increase belowground CO_2 efflux, which should be considered together with ecosystem productivity and net C balance when evaluating bamboo forests as C sinks (Natori and Hino, 2021; Yamamoto and Inoue, 2023). Previous studies have consistently shown that fine-roots exhibit much higher mass-specific respiration rates than coarse-roots owing to their smaller diameter and higher metabolic activity (Desrochers et al., 2002; Makita et al., 2012; Marsden et al., 2008). However, because coarse-roots constitute a large fraction of belowground biomass, their contribution to autotrophic respiration can be substantial at the stand scale, which explains the relatively high coarse-root contribution observed in the deciduous forest in this study.

Although T_s was a more consistent predictor of R_a than θ, the weak θ effect should not be interpreted as general insensitivity of root respiration to soil moisture. Both variables were monitored continuously, but R_a was measured during eight field campaigns, and seasonal covariation between T_s and θ may have limited the detection of their independent effects. Thus, T_s was the dominant predictor under the conditions observed in this study, whereas the role of θ under stronger moisture limitation remains uncertain.

The Q_{10} values for fine-root respiration were 2.1–2.6 in BF, CF, and DF, respectively. These values fell within the broad range reported for forest root respiration, including 2.4–3.1 across diverse US forests and 1.1–2.0 across root orders and soil depths in six temperate tree species (Burton et al., 2002; Wang et al., 2023). Previous studies in Moso bamboo forests have reported Q_{10} values of 1.2 for root respiration and 4.1 for total soil respiration, indicating that estimated temperature sensitivity varies with the respiratory component and measurement approach (Hsieh et al., 2016; Tang et al., 2015).

Shapley contribution analysis clarified the mechanisms underlying the differences in R_a among the forest types (Fig. 5). In the CF-to-BF comparison, R_a increased by approximately 400%, despite a large negative contribution from the fine-root physiological parameter (k_f; −100%). This net increase was primarily driven by the strong positive contribution of fine-root biomass (W_f; +400%), with additional positive contributions from the fine-root parameter j_f, W_c, (+50%), and T_s (+10%). Together, these positive effects outweighed the negative influence of b_f and other minor terms, indicating that the pronounced increase in R_a in BF than CF was associated primarily with fine-root biomass accumulation rather than enhanced root-level physiological activity (Hirano et al., 2023; Lloyd and Taylor, 1994).

In the DF-to-BF comparison, the net change in R_a was small, despite a substantial positive contribution from W_f (+80%). In this case, the positive effect of W_f was largely counterbalanced by negative contributions from fine-root physiological parameters (j_f and k_f; −20%–25%) and W_c (−20%), whereas soil temperature and coarse-root physiological parameters contributed only small positive contributions. As a result, these offsetting effects resulted in similar annual R_a between the bamboo and broad-leaved stands, demonstrating that contrasting combinations of fine-root biomass and mass-specific respiration can produce comparable stand-level outcomes despite substantial differences in root-system structure (Cui et al., 2021).

Together, these findings indicate that the factors associated with R_a differences among the three adjacent stands were context dependent. At our study site, the higher R_a in BF than in CF was primarily associated with greater fine-root biomass, whereas the similar R_a between BF and DF resulted from compensating biomass and physiological effects. These contrasting patterns suggest that R_a responses associated with bamboo expansion may depend on the root biomass and physiological characteristics of the adjacent forest. In the comparison with the cedar stand, fine-root biomass accumulation was the main factor associated with higher R_a in BF. In contrast, in the comparison with the broad-leaved stand, biomass and physiological effects largely offset one another, resulting in little difference in annual R_a. These site-specific patterns highlight the importance of considering both biomass-related and physiological traits when assessing how bamboo expansion may influence belowground C dynamics within SEPLs.

4.3. Implications

This study has several limitations that should be addressed to translate our findings into management-relevant assessments of C dynamics in expanding bamboo forests. First, although the soil core method enabled explicit separation of fine- and coarse-root contributions to R_a, it inevitably involved root excision and disturbance, which

may bias absolute respiration rates and limit representation of in situ root activity (Makita et al., 2013; Marsden et al., 2008; Rakonczay et al., 1997). The 10-cm-diameter soil cores may have underrepresented large structural roots. Rhizomes were rarely encountered despite repeated soil-core sampling, but their low occurrence and small contribution to R_a within the sampled cores should not be regarded as evidence of a negligible contribution at the stand scale. Moso bamboo rhizomes have been reported to occur mainly within the 10–30 cm soil layer (Li et al., 2021). Moreover, previous studies have shown that rhizomes represent an important component of belowground C production and respiration in Moso bamboo forests (Kobayashi et al., 2023; Lv et al., 2025). Because sampling was restricted to a depth of 0–20 cm, the observed contribution of rhizomes should not be extrapolated to the entire bamboo stand. R_a also excluded rhizosphere and mycorrhizal respiration and should therefore be interpreted as respiration measured from extracted roots rather than total ecosystem-scale autotrophic respiration.

Second, each forest type was represented by a single stand. Therefore, the present results should be interpreted as a local comparison among adjacent stands rather than as broadly representative of SEPLs in the region. Further studies across multiple sites and geographic regions are needed to assess the general applicability of the observed patterns. Third, because this study focused on belowground C efflux and did not quantify net ecosystem productivity (NEP), we were unable to determine whether the high R_a observed in bamboo forest results in net C loss or is compensated by high primary productivity at the ecosystem scale (Kume et al., 2025).

Addressing these limitations in an integrated manner will be critical for advancing both scientific understanding and practical decision-making (Bond-Lamberty et al., 2024; Kuzyakov, 2006). Future studies should combine core-based partitioning with continuous and less invasive measurements of soil respiration, such as automated chamber systems, to constrain disturbance effects and better capture temporal variability (Bond-Lamberty et al., 2024; Giasson et al., 2013; Phillips et al., 2017). In addition, belowground flux measurements need to be embedded within a full ecosystem C budget by incorporating aboveground productivity, biomass accumulation, litter inputs, and heterotrophic respiration (Bond-Lamberty and Thomson, 2010; Pan et al., 2011; Raich and Schlesinger, 1992). Integrating plot-scale inventories with ecosystem-scale approaches, such as eddy-covariance or repeated biomass censuses, would allow direct estimation of NEP and clarify the interaction between increased autotrophic respiration and bamboo productivity (Kume et al., 2025; Luyssaert et al., 2007).

Such integrated assessments are essential for evaluating whether bamboo expansion should be actively managed and, if so, how management strategies should be designed (Natori and Hino, 2021; Suzuki and Nakagoshi, 2011). In SEPLs, management objectives extend beyond preventing forest-type conversion and instead focus on sustaining multiple ecosystem services, including C sequestration (Duraiappah, 2012; Natori and Hino, 2021; Takeuchi et al., 2016). By linking changes in belowground CO_2 efflux associated with bamboo expansion to ecosystem-scale net C balance (NEP), future studies can determine whether increased CO_2 efflux contributes to net C loss or is offset by high primary productivity (Kume et al., 2025; Lin et al., 2017; Tang et al., 2016a). This distinction is important for deciding when bamboo expansion should be controlled and when bamboo-dominated stands may be tolerated. Based on the local results of this study, active control may be needed when bamboo expands into stands with low root biomass, such as the Japanese cedar stand examined here, and substantially increases fine-root biomass and root-derived CO_2 efflux. Control may also be appropriate when maintaining the original forest structure or other ecosystem services is an important management goal. In contrast, bamboo expansion may be tolerated with continued monitoring when annual R_a does not increase substantially, as observed in the broad-leaved stand examined here. However, management decisions should also consider NEP, biodiversity, and other ecosystem services that were not evaluated in this study.

Ultimately, improving our ability to evaluate net C outcomes will support the development of management options that enhance C sequestration while maintaining the multifunctionality of SEPLs. Rather than applying uniform control measures, evidence-based assessments should be used to determine whether bamboo expansion requires active suppression, continued monitoring, or partial regulation. Context-specific strategies may include regulating bamboo density or spatial extent where expansion substantially increases belowground CO_2 efflux or conflicts with forest-structure objectives, while tolerating bamboo-dominated stands where net C balance and other ecosystem services are maintained (Deng et al., 2020; Suzuki and Nakagoshi, 2011). Resolving the methodological and conceptual limitations identified here will directly contribute to more effective and adaptive management of bamboo expansion in human-influenced forest landscapes.

5. List of abbreviations

T_s: soil temperature (°C)
θ: soil volumetric water content (%)
R_s: soil respiration (g CO_2 m^{-2} h^{-1}) = $R_h + R_a$
R_h: heterotrophic respiration (g CO_2 m^{-2} h^{-1})
R_a: autotrophic respiration (g CO_2 m^{-2} h^{-1}) = $R_{a_f} + R_{a_c}$
R_{a_f}: fine-root respiration
R_{a_c}: coarse-root respiration
W: total root dry mass (g cm^{-2})
W_f: fine-root dry mass (g cm^{-2})
W_c: coarse-root dry mass (g cm^{-2})

Declaration of generative AI and AI-assisted technologies in the manuscript preparation process

During the preparation of this work the authors used Nano Banana Pro (URL: https://gemini.google/jp/overview/image-generation) in order to make illustration in Fig. 5a-c. After using this tool, the authors reviewed and edited the content as needed and take full responsibility for the content of the published article.

CRediT authorship contribution statement

Kousuke Nagai: Writing – review & editing, Writing – original draft, Formal analysis, Data curation, Conceptualization. **Si Ho Han:** Writing – review & editing, Writing – original draft, Visualization, Software, Formal analysis, Conceptualization. **Dongchuan Fu:** Writing – review & editing, Writing – original draft, Methodology, Investigation, Formal analysis, Data curation. **Hayato Abe:** Writing – review & editing, Writing – original draft, Visualization, Supervision, Software, Methodology. **Tomonori Kume:** Writing – review & editing, Writing – original draft, Supervision, Project administration, Funding acquisition, Conceptualization.

Declaration of competing interest

The authors declare the following financial interests/personal relationships which may be considered as potential competing interests: Si Ho Han reports financial support was provided by Japan Society for the Promotion of Science. Tomonori Kume reports financial support was provided by Japan Society for the Promotion of Science. If there are other authors, they declare that they have no known competing financial interests or personal relationships that could have appeared to influence the work reported in this paper.

Acknowledgments

This study was supported by JSPS KAKENHI (Grant Numbers 23K27043, 21H05316, 22KK0168 and 25KF0255). We sincerely thank Dr. Mizue Ohashi (Hyogo University) and Dr. Ayumi Katayama (Kyushu

University, Japan) for their valuable technical advice. Also, We thank Dr. Robert McKenzie, from Edanz (https://jp.edanz.com/ac) for editing the English text of a draft of this manuscript.

Supplementary materials

Supplementary material associated with this article can be found, in the online version, at doi:10.1016/j.agrformet.2026.111525.

Data availability

Data will be made available on request.

References

Abe, H., Kume, T., Katayama, A., 2025. Soil respiration and heterotrophic respiration in a cool-temperate forest with sika deer-induced alteration of understory vegetation. J. Agric. Meteorol. 81, 152–163. https://doi.org/10.2480/agrmet.D-24-00032.

An, J.Y., Park, B.B., Chun, J.H., Osawa, A., 2017. Litterfall production and fine root dynamics in cool-temperate forests. PLOS ONE 12, e0180126. https://doi.org/10.1371/journal.pone.0180126.

Anjos, L., Gaistardo, C.C., Deckers, J., Dondeyne, S., Eberhardt, E., Gerasimova, M., Harms, B., Jones, A., Krasilnikov, P., Reinsch, T., Vargas, R., Zhang, G.-L., 2015. World Reference Base For Soil Resources 2014 International soil Classification System For Naming Soils and Creating Legends For Soil Maps [WWW Document]. JRC Publ. ReposURL. https://publications.jrc.ec.europa.eu/repository/handle/JRC91947. accessed 12.27.25.

Benton, A., 2015. Priority species of bamboo. In: Liese, W., Köhl, M. (Eds.), Bamboo: The Plant and Its Uses. Springer International Publishing, Cham, pp. 31–41. https://doi.org/10.1007/978-3-319-14133-6_2.

Bond-Lamberty, B., Ballantyne, A., Berryman, E., Fluet-Chouinard, E., Jian, J., Morris, K. A., Rey, A., Vargas, R., 2024. Twenty years of progress, challenges, and opportunities in measuring and understanding soil respiration. J. Geophys. Res. Biogeosciences 129, e2023JG007637. https://doi.org/10.1029/2023JG007637.

Bond-Lamberty, B., Thomson, A., 2010. A global database of soil respiration data. Biogeosciences 7, 1915–1926. https://doi.org/10.5194/bg-7-1915-2010.

Bouma, T.J., Nielsen, K.L., Eissenstat, D.M., Lynch, J.P., 1997. Estimating respiration of roots in soil: interactions with soil CO_2, soil temperature and soil water content. Plant Soil 195, 221–232. https://doi.org/10.1023/A:1004278421334.

Burton, A., Pregitzer, K., Ruess, R., Hendrick, R., Allen, M., 2002. Root respiration in North American forests: effects of nitrogen concentration and temperature across biomes. Oecologia 131, 559–568. https://doi.org/10.1007/s00442-002-0931-7.

Burton, A.J., Pregitzer, K.S., Zogg, G.P., Zak, D.R., 1998. Drought reduces root respiration in sugar maple forests. Ecol. Appl. 8, 771–778. https://doi.org/10.1890/1051-0761(1998)008%5B0771:DRRRIS%5D2.0.CO;2.

Chen, Z., Xu, Y., Fan, J., Yu, H., Ding, W., 2017. Soil autotrophic and heterotrophic respiration in response to different N fertilization and environmental conditions from a cropland in Northeast China. Soil Biol. Biochem. 110, 103–115. https://doi.org/10.1016/j.soilbio.2017.03.011.

Clark, L.G., Londoño, X., Ruiz-Sanchez, E., 2015. Bamboo taxonomy and habitat. Eds.. In: Liese, W., Köhl, M. (Eds.), Bamboo: The Plant and Its Uses. Springer International Publishing, Cham, pp. 1–30. https://doi.org/10.1007/978-3-319-14133-6_1.

Cui, R., Hirano, T., Sun, L., Teramoto, M., Liang, N., 2021. Variations in biomass, production and respiration of fine roots in a young larch forest. J. Agric. Meteorol. 77, 167–178. https://doi.org/10.2480/agrmet.D-20-00049.

Deng, X., Yin, J., Xu, L., Shi, Y., Zhou, G., Li, Y., Chen, G., Ye, Y., Zhang, F., Zhou, Y., Xiong, Y., 2020. Effects of abandonment management on soil C and N pools in Moso bamboo forests. Sci. Total Environ. 729, 138949. https://doi.org/10.1016/j.scitotenv.2020.138949.

Desrochers, A., Landhausser, S.M., Lieffers, V.J., 2002. Coarse and fine root respiration in aspen (Populus tremuloides). Tree Physiol. 22, 725–732. https://doi.org/10.1093/treephys/22.10.725.

Duraiappah, A.K., 2012. Computational Models in the Economics of Environment and Development. Springer Science & Business Media.

Ewel, K.C., Cropper Jr, W.P., Gholz, H.L., 1987. Soil CO2 evolution in Florida slash pine plantations. II. Importance of root respiration. Can. J. For. Res. 17, 330–333. https://doi.org/10.1139/x87-055.

Fernando, M., 2020. nlraa: nonlinear Regression for agricultural applications. CRAN Contrib. Packag.. https://doi.org/10.32614/cran.package.nlraa.

Forster, D., Harrison, M.T., Adachi, M., 2025. Uncovering environmental implications of historical stewardship of Japanese Moso Bamboo (*Phyllostachys edulis*) forests: a review using a multivariate imputation approach. Ecol. Inform. 90, 103348. https://doi.org/10.1016/j.ecoinf.2025.103348.

Fukushima, K., Usui, N., Ogawa, R., Tokuchi, N., 2015. Impacts of moso bamboo (Phyllostachys pubescens) invasion on dry matter and carbon and nitrogen stocks in a broad-leaved secondary forest located in Kyoto, western Japan. Plant Species Biol. 30, 81–95. https://doi.org/10.1111/1442-1984.12066.

Giasson, M.-A., Ellison, A.M., Bowden, R.D., Crill, P.M., Davidson, E.A., Drake, J.E., Frey, S.D., Hadley, J.L., Lavine, M., Melillo, J.M., Munger, J.W., Nadelhoffer, K.J., Nicoll, L., Ollinger, S.V., Savage, K.E., Steudler, P.A., Tang, J., Varner, R.K., Wofsy, S.C., Foster, D.R., Finzi, A.C., 2013. Soil respiration in a northeastern US temperate forest: a 22-year synthesis. Ecosphere 4, art140. https://doi.org/10.1890/ES13.00183.1.

Han, S.H., Carayugan, M.B., An, J.Y., Youn, W.B., Kume, T., Park, B.B., 2026. Evaluating stand structural and functional impacts of understory removal in forests dominated by low-nutrient specialists in South Korea. Ecol. Indic. 184, 114730. https://doi.org/10.1016/j.ecolind.2026.114730.

Hirano, T., Cui, R., Sun, L., Teramoto, M., Liang, N., 2023. Partitioning of root respiration into growth, maintenance, and ion uptake components in a young larch-dominated forest. Plant Soil 482, 57–72. https://doi.org/10.1007/s11104-022-05674-0.

Hothorn, T., Bretz, F., Westfall, P., 2008. Simultaneous inference in general parametric models. Biom. J. 50, 346–363. https://doi.org/10.1002/bimj.200810425.

Hsieh, I.-F., Kume, T., Lin, M.-Y., Cheng, C.-H., Miki, T., 2016. Characteristics of soil CO_2 efflux under an invasive species, Moso bamboo, in forests of central Taiwan. Trees 30, 1749–1759. https://doi.org/10.1007/s00468-016-1405-6.

Hu, S., Li, Y., Chang, S.X., Li, Y., Yang, W., Fu, W., Liu, J., Jiang, P., Lin, Z., 2018. Soil autotrophic and heterotrophic respiration respond differently to land-use change and variations in environmental factors. Agric. For. Meteorol. 290–298. https://doi.org/10.1016/j.agrformet.2018.01.003, 250–251.

Huang, K., Li, Yongfu, Hu, J., Tang, C., Zhang, S., Fu, S., Jiang, P., Ge, T., Luo, Y., Song, X., Li, Y., Cai, Y., 2021. Rates of soil respiration components in response to inorganic and organic fertilizers in an intensively-managed Moso bamboo forest. Geoderma 403, 115212. https://doi.org/10.1016/j.geoderma.2021.115212.

Ichihashi, R., Chiu, C.-W., Komatsu, H., Kume, T., Shinohara, Y., Tateishi, M., Tsuruta, K., Otsuki, K., 2017. Contribution of lianas to community-level canopy transpiration in a warm-temperate forest. Funct. Ecol. 31, 1690–1699. https://doi.org/10.1111/1365-2435.12881.

Ichihashi, R., Komatsu, H., Kume, T., Onozawa, Y., Shinohara, Y., Tsuruta, K., Otsuki, K., 2015. Stand-scale transpiration of two Moso bamboo stands with different culm densities. Ecohydrology 8, 450–459. https://doi.org/10.1002/eco.1515.

Isagi, Y., Torii, A., 1997. Range expansion and its mechanisms in a naturalized bamboo species, Phyllostachys pubescens. Japan. J. Sustain. For. 6, 127–141. https://doi.org/10.1300/J091v06n01_08.

Jarvi, M.P., Burton, A.J., 2020. Root respiration and biomass responses to experimental soil warming vary with root diameter and soil depth. Plant Soil 451, 435–446. https://doi.org/10.1007/s11104-020-04540-1.

Jassal, R.S., Black, T.A., 2006. Estimating heterotrophic and autotrophic soil respiration using small-area trenched plot technique: theory and practice. Agric. For. Meteorol. Fluxnet-Canada Res. Netw. 140, 193–202. https://doi.org/10.1016/j.agrformet.2005.12.012.

Jian, J., Vargas, R., Anderson-Teixeira, K., Stell, E., Herrmann, V., Horn, M., Kholod, N., Manzon, J., Marchesi, R., Paredes, D., Bond-Lamberty, B., 2021. A restructured and updated global soil respiration database (SRDB-V5). Earth Syst. Sci. Data 13, 255–267. https://doi.org/10.5194/essd-13-255-2021.

Jiang, H., Deng, Q., Zhou, G., Hui, D., Zhang, D., Liu, S., Chu, G., Li, J., 2013. Responses of soil respiration and its temperature/moisture sensitivity to precipitation in three subtropical forests in southern China. Biogeosciences 10, 3963–3982. https://doi.org/10.5194/bg-10-3963-2013.

Jiao, J., Cheng, Y., Hong, P., Ma, J., Yao, L., Jiang, B., Xu, X., Wu, C., 2024. Impact of Fragmentation on Carbon Uptake in Subtropical Forest Landscapes in Zhejiang Province, 16. Remote Sens, China, p. 2393. https://doi.org/10.3390/rs16132393.

Kobayashi, K., Ohashi, M., Fujihara, M., Kitayama, K., Onoda, Y., 2023. Rhizomes play significant roles in biomass accumulation, production and carbon turnover in a stand of the tall bamboo Phyllostachys edulis. J. For. Res. 28, 42–50. https://doi.org/10.1080/13416979.2022.2090669.

Kume, T., Lin, P.-H., Orrego, M., Chung, M.-H., Laplace, S., Han, S.-H., 2025. Inconsistent interannual variations between net primary production and soil CO_2 effluxes in a Moso bamboo forest. J. For. Res. 30, 234–241. https://doi.org/10.1080/13416979.2024.2440993.

Kuzyakov, Y., 2006. Sources of CO2 efflux from soil and review of partitioning methods. Soil Biol. Biochem. 38, 425–448. https://doi.org/10.1016/j.soilbio.2005.08.020.

Kuzyakov, Y., Larionova, A.A., 2005. Root and rhizomicrobial respiration: a review of approaches to estimate respiration by autotrophic and heterotrophic organisms in soil. J. Plant Nutr. Soil Sci. 168, 503–520. https://doi.org/10.1002/jpln.200421703.

Li, C., Cai, Y., Xiao, L., Gao, X., Shi, Y., Zhou, Y., Du, H., Zhou, G., 2021. Rhizome extension characteristics, structure and carbon storage relationships with culms in a 10-year moso bamboo reforestation period. For. Ecol. Manag. 498, 119556. https://doi.org/10.1016/j.foreco.2021.119556.

Li, X., Guo, D., Zhang, C., Niu, D., Fu, H., Wan, C., 2018. Contribution of root respiration to total soil respiration in a semi-arid grassland on the Loess Plateau. China. Sci. Total Environ. 627, 1209–1217. https://doi.org/10.1016/j.scitotenv.2018.01.313.

Lin, M.-Y., Hsieh, I.-F., Lin, P.-H., Laplace, S., Ohashi, M., Chen, T.-H., Kume, T., 2017. Moso bamboo (Phyllostachys pubescens) forests as a significant carbon sink? A case study based on 4-year measurements in central Taiwan. Ecol. Res. 32, 845–857. https://doi.org/10.1007/s11284-017-1497-5.

Lindstrom, M.J., Bates, D.M., 1990. Nonlinear mixed effects models for repeated measures data. Biometrics 46, 673–687. https://doi.org/10.2307/2532087.

Liu, J., Jiang, P., Wang, H., Zhou, G., Wu, J., Yang, F., Qian, X., 2011. Seasonal soil CO_2 efflux dynamics after land use change from a natural forest to Moso bamboo plantations in subtropical China. For. Ecol. Manag. 262, 1131–1137. https://doi.org/10.1016/j.foreco.2011.06.015.

Lloyd, J., Taylor, J.A., 1994. On the temperature dependence of soil respiration. Funct. Ecol. 8, 315–323. https://doi.org/10.2307/2389824.

Luyssaert, S., Inglima, I., Jung, M., Richardson, A.D., Reichstein, M., Papale, D., Piao, S. L., Schulze, E.-D., Wingate, L., Matteucci, G., Aragao, L., Aubinet, M., Beer, C., Bernhofer, C., Black, K.G., Bonal, D., Bonnefond, J.-M., Chambers, J., Ciais, P., Cook, B., Davis, K.J., Dolman, A.J., Gielen, B., Goulden, M., Grace, J., Granier, A., Grelle, A., Griffis, T., Grünwald, T., Guidolotti, G., Hanson, P.J., Harding, R., Hollinger, D.Y., Hutyra, L.R., Kolari, P., Kruijt, B., Kutsch, W., Lagergren, F.,

Laurila, T., Law, B.E., Le Maire, G., Lindroth, A., Loustau, D., Malhi, Y., Mateus, J., Migliavacca, M., Misson, L., Montagnani, L., Moncrieff, J., Moors, E., Munger, J.W., Nikinmaa, E., Ollinger, S.V., Pita, G., Rebmann, C., Roupsard, O., Saigusa, N., Sanz, M.J., Seufert, G., Sierra, C., Smith, M.-L., Tang, J., Valentini, R., Vesala, T., Janssens, I.A., 2007. CO2 balance of boreal, temperate, and tropical forests derived from a global database. Glob. Change Biol. 13, 2509–2537. https://doi.org/10.1111/j.1365-2486.2007.01439.x.

Lv, J., Li, Q., Cao, T., Shi, M., Peng, C., Deng, L., Song, X., 2025. A compartmentation approach to deconstruct ecosystem carbon fluxes of a Moso bamboo forest in subtropical China. For. Ecosyst. 12, 100286. https://doi.org/10.1016/j.fecs.2024.100286.

Ma, L., Shen, C., Lou, D., Fu, S., Guan, D., 2017. Ecosystem carbon storage in forest fragments of differing patch size. Sci. Rep. 7, 13173. https://doi.org/10.1038/s41598-017-13598-4.

Majdi, H., Nylund, J.-E., Ågren, G.I., 2007. Root respiration data and minirhizotron observations conflict with root turnover estimates from sequential soil coring. Scand. J. For. Res. 22, 299–303. https://doi.org/10.1080/02827580701346353.

Makita, N., Kosugi, Y., Dannoura, M., Takanashi, S., Niiyama, K., Kassim, A.R., Nik, A.R., 2012. Patterns of root respiration rates and morphological traits in 13 tree species in a tropical forest. Tree Physiol. 32, 303–312. https://doi.org/10.1093/treephys/tps008.

Makita, N., Yaku, R., Ohashi, M., Fukuda, K., Ikeno, H., Hirano, Y., 2013. Effects of excising and washing treatments on the root respiration rates of Japanese cedar (Cryptomeria japonica) seedlings. J. For. Res. 18, 379–383. https://doi.org/10.1007/s10310-012-0355-0.

Marsden, C., Nouvellon, Y., Epron, D., 2008. Relating coarse root respiration to root diameter in clonal Eucalyptus stands in the Republic of the Congo. Tree Physiol. 28, 1245–1254. https://doi.org/10.1093/treephys/28.8.1245.

Mauritz, M., Lipson, D.A., 2021. Plant community composition alters moisture and temperature sensitivity of soil respiration in semi-arid shrubland. Oecologia 197, 1003–1015. https://doi.org/10.1007/s00442-021-04961-4.

Natori, Y., Hino, A., 2021. Global identification and mapping of socio-ecological production landscapes with the Satoyama Index. PLOS ONE 16, e0256327. https://doi.org/10.1371/journal.pone.0256327.

Nishikawa, R., Murakami, T., Yoshida, S., Mitsuda, Y., Nagashima, K., Mizoue, N., 2005. Characteristic of temporal range shifts of bamboo stands according to adjacent landcover type. J. Jpn. For. Soc. 87, 402–409. https://doi.org/10.4005/jjfs.87.402.

Pan, Y., Birdsey, R.A., Fang, J., Houghton, R., Kauppi, P.E., Kurz, W.A., Phillips, O.L., Shvidenko, A., Lewis, S.L., Canadell, J.G., Ciais, P., Jackson, R.B., Pacala, S.W., McGuire, A.D., Piao, S., Rautiainen, A., Sitch, S., Hayes, D., 2011. A large and persistent carbon sink in the world's forests. Science 333, 988–993. https://doi.org/10.1126/science.1201609.

Phillips, C.L., Bond-Lamberty, B., Desai, A.R., Lavoie, M., Risk, D., Tang, J., Todd-Brown, K., Vargas, R., 2017. The value of soil respiration measurements for interpreting and modeling terrestrial carbon cycling. Plant Soil 413, 1–25. https://doi.org/10.1007/s11104-016-3084-x.

Pinheiro, J., Bates, D., R Core Team, 2022. nlme: Linear and Nonlinear Mixed Effects Models. https://doi.org/10.32614/CRAN.package.nlme.

Pregitzer, K.S., Laskowski, M.J., Burton, A.J., Lessard, V.C., Zak, D.R., 1998. Variation in sugar maple root respiration with root diameter and soil depth. Tree Physiol. 18, 665–670. https://doi.org/10.1093/treephys/18.10.665.

R Core Team, 2024. A language and environment for statistical computing. R Found. Statist. Comput. https://www.R-project.org/.

Raich, J.W., Schlesinger, W.H., 1992. The global carbon dioxide flux in soil respiration and its relationship to vegetation and climate. Tellus B 44, 81–99. https://doi.org/10.1034/j.1600-0889.1992.t01-1-00001.x.

Rakonczay, Z., Seiler, J.R., Samuelson, L.J., 1997. A method for the in situ measurement of fine root gas exchange of forest trees. Environ. Exp. Bot. 37, 107–113. https://doi.org/10.1016/S0098-8472(96)01048-9.

Saiz, G., Byrne, K.A., Butterbach-Bahl, K., Kiese, R., Blujdea, V., Farrell, E.P., 2006. Stand age-related effects on soil respiration in a first rotation Sitka spruce chronosequence in central Ireland. Glob. Change Biol. 12, 1007–1020. https://doi.org/10.1111/j.1365-2486.2006.01145.x.

Shi, B., Gao, W., Jin, G., 2015. Effects on rhizospheric and heterotrophic respiration of conversion from primary forest to secondary forest and plantations in northeast China. Eur. J. Soil Biol. 66, 11–18. https://doi.org/10.1016/j.ejsobi.2014.11.003.

Shimono, K., Katayama, A., Kume, T., Enoki, T., Chiwa, M., Hishi, T., 2022. Differences in net primary production allocation and nitrogen use efficiency between Moso bamboo and Japanese cedar forests along a slope. J. For. Res. 27, 28–35. https://doi.org/10.1080/13416979.2021.1965280.

Shinohara, Y., Kume, T., Ichihashi, R., Komatsu, H., Otsuki, K., 2014. Moso-bamboo Forests in Japan: J. Jpn. For. Soc. 96, 351–361. https://doi.org/10.4005/jjfs.96.351.

Shinohara, Y., Misumi, Y., Kubota, T., Nanko, K., 2019. Characteristics of soil erosion in a moso-bamboo forest of western Japan: comparison with a broadleaved forest and a coniferous forest. CATENA 172, 451–460. https://doi.org/10.1016/j.catena.2018.09.011.

Soga, M., Gaston, K.J., 2016. Extinction of experience: the loss of human–nature interactions. Front. Ecol. Environ. 14, 94–101. https://doi.org/10.1002/fee.1225.

Spiess, A.-N., Neumeyer, N., 2010. An evaluation of R2 as an inadequate measure for nonlinear models in pharmacological and biochemical research: a Monte Carlo approach. BMC Pharmacol. 10 (6). https://doi.org/10.1186/1471-2210-10-6.

Suzuki, S., Nakagoshi, N., 2011. Sustainable management of Satoyama Bamboo landscapes in Japan. In: Hong, S.-K., Kim, J.-E., Wu, J., Nakagoshi, N. (Eds.), Landscape Ecology in Asian Cultures. Springer, Japan, Tokyo, pp. 211–220. https://doi.org/10.1007/978-4-431-87799-8_15.

Takeuchi, R., Wahyudi, I., Aiso, H., Ishiguri, F., Tyas Istikowati, W., Ohkubo, T., Ohshima, J., Iizuka, K., Yokota, S., 2016. Wood properties related to pulp and paper quality in two Macaranga species naturally regenerated in secondary forests, Central Kalimantan, Indonesia. Tropics 25, 107–115. https://doi.org/10.3759/tropics.MS15-23.

Tang, X., Fan, S., Qi, L., Guan, F., Du, M., Zhang, H., 2016a. Soil respiration and net ecosystem production in relation to intensive management in Moso bamboo forests. CATENA 137, 219–228. https://doi.org/10.1016/j.catena.2015.09.008.

Tang, X., Fan, S., Qi, L., Guan, F., Liu, G., Du, M., 2015. Effects of understory removal on root production, turnover and total belowground carbon allocation in Moso bamboo forests. IForest - Biogeosci. For. 9, 187–194. https://doi.org/10.3832/ifor1674-008.

Tang, X., Fan, S., Qi, L., Guan, F., Su, W., Du, M., 2016b. A comparison of soil respiration, carbon balance and root carbon use efficiency in two managed Moso bamboo forests in subtropical China. Ann. For. Res. 59, 3–20. https://doi.org/10.15287/afr.2016.497.

Thurgood, A., Singh, B., Jones, E., Barbour, M.M., 2014. Temperature sensitivity of soil and root respiration in contrasting soils. Plant Soil 382, 253–267. https://doi.org/10.1007/s11104-014-2159-9.

Torii, A., 1998. Estimation of range expansion rate of bamboo stands using aerial photographs : case study on Mt. Hachiman, Shiga Prefecture, and Mt. Otoko, Kyoto Prefecture, Japan. Jpn. J. Ecol. 48, 37–47. https://doi.org/10.18960/seitai.48.1_37.

Torii, A., 2003. Bamboo stands are expanding and invading adjacent forests in "Satoyama. J. Jpn. Soc. Reveg. Technol. 28, 412–416. https://doi.org/10.7211/jjsrt.28.412.

Torii, A., Isagi, Y., 1997. Range expansion of bamboo species in southern areas of Kyoto Prefecture. Japan. Jpn. J. Ecol. 47, 31–41. https://doi.org/10.18960/seitai.47.1_31.

Tu, L., Hu, T., Zhang, J., Li, X., Hu, H., Liu, L., Xiao, Y., 2013. Nitrogen addition stimulates different components of soil respiration in a subtropical bamboo ecosystem. Soil Biol. Biochem. 58, 255–264. https://doi.org/10.1016/j.soilbio.2012.12.005.

Vogt, K., Persson, H., 1991. Measuring growth and development of roots. Meas. Growth Dev. Roots Tech. Approaches For. Tree Ecophysiol. 477–501.

Wadoux, A.M.J.-C., 2023. Interpretable spectroscopic modelling of soil with machine learning. Eur. J. Soil Sci. 74, e13370. https://doi.org/10.1111/ejss.13370.

Wang, D., Gao, G., Wang, Y., Jia, S., Gu, J., 2023. Temperature sensitivity of root respiration declines with increasing soil depth in six temperate tree species. Plant Soil 492, 315–328. https://doi.org/10.1007/s11104-023-06176-3.

Xu, Y., Jiao, J., Wu, C., Zhao, Z., Ge, X., Gao, G., Cao, Y., Zhou, B., 2024. Abandonment leads to changes in forest structural and soil organic carbon stocks in moso bamboo forests. Plants 13, 2301. https://doi.org/10.3390/plants13162301.

Yamamoto, M., Inoue, A., 2023. Predicting changes in the carbon stocks of bamboo forests in Japan from 1985 to 2005. J. For. Res. 28, 407–415. https://doi.org/10.1080/13416979.2023.2229984.

Yamauchi, K., Tashiro, N., Chiwa, M., Katayama, A., Nanki, D., Fujiyama, M., Taketo, O., Nakamura, T., Ougi, D., Murata, S., Kume, T., 2026. Characteristics of meteorological observation data from Kyushu University's three research forests. Bull. Kyushu Univ. For. 107, 7–15. https://doi.org/10.15017/7420539.

Yen, T.-M., Ji, Y.-J., Lee, J.-S., 2010. Estimating biomass production and carbon storage for a fast-growing makino bamboo (*Phyllostachys makinoi*) plant based on the diameter distribution model. For. Ecol. Manag. 260, 339–344. https://doi.org/10.1016/j.foreco.2010.04.021.

Zhang, X., Zhao, T., Xu, H., Liu, W., Wang, J., Chen, X., Liu, L., 2024. GLC_FCS30D: the first global 30 m land-cover dynamics monitoring product with a fine classification system for the period from 1985 to 2022 generated using dense-time-series Landsat imagery and the continuous change-detection method. Earth Syst. Sci. Data 16, 1353–1381. https://doi.org/10.5194/essd-16-1353-2024.